HHS Public Access

Author manuscript

Environ Sci Pollut Res Int. Author manuscript; available in PMC 2021 August 01.

Published in final edited form as:

Environ Sci Pollut Res Int. 2020 August ; 27(24): 30542–30557. doi:10.1007/s11356-020-09257-3.

Environmental risk mapping of potential abandoned uranium mine contamination on the Navajo Nation, USA, using a GIS-based multi-criteria decision analysis approach

Yan Lin[1,*], **Joseph Hoover**[2], **Daniel Beene**[3], **Esther Erdei**[4], **Zhuoming Liu**[5]

[1]Department of Geography and Environmental Studies, University of New Mexico, Albuquerque, NM, USA

[2]Department of Social Sciences and Cultural Studies, Montana State University Billings, Billings, MT, USA

[3]Community Environmental Health Program, College of Pharmacy, Health Sciences Center, University of New Mexico, Albuquerque, NM, USA

[4]Community Environmental Health Program, College of Pharmacy, Health Sciences Center, University of New Mexico, Albuquerque, NM, USA

[5]Department of Geography and Environmental Studies, University of New Mexico, Albuquerque, NM, USA

Abstract

The Navajo Nation (NN), a sovereign indigenous tribal nation in the Southwestern United States, is home to 523 abandoned uranium mines (AUMs). Previous health studies have articulated numerous human health hazards associated with AUMs and multiple environmental mechanisms/pathways (e.g. air, water, and soil) for contaminant transport. Despite this evidence, the limited modeling of AUM contamination that exists relies solely on proximity to mines and only considers single rather than combined pathways from which the contamination is a product. In order to better understand the spatial dynamics of contaminant exposure across the NN, we adopted the following established geospatial and computational methods to develop a more sophisticated environmental risk map illustrating the potential for AUM contamination: GIS-based multi-criteria decision analysis (GIS-MCDA), fuzzy logic, and analytic hierarchy process (AHP). Eight criteria layers were selected for the GIS-MCDA model: proximity to AUMs, roadway proximity, drainage proximity, topographic landforms, wind index, topographic wind exposure, vegetation index, and groundwater contamination. Model sensitivity was evaluated using the one-at-a-time method and statistical validation analysis was conducted using two separate environmental datasets. The sensitivity analysis indicated consistency and reliability of the model. Model results were strongly associated with environmental uranium concentrations. The model classifies 20.2% of the NN as high potential for AUM contamination while 65.7% and 14.1% of the region are at medium and low risk, respectively. This study is entirely a novel application and a crucial first step toward

[*]corresponding author yanlin@unm.edu, (505)-277-0877.

Data sharing statement

Python codes used in the analysis of this work are available in a Git repository: https://github.com/dbeene/OATsensitivity

informing future epidemiologic studies and ongoing remediation efforts to reduce human exposure to AUM waste.

Keywords

Multi-criteria decision analysis; abandoned uranium mines; environmental risk mapping; Navajo Nation; weighted linear combination; analytic hierarchy process

Introduction

Abandoned hard rock mines are prevalent throughout the western United States (Government Accountability Office 2011). These abandoned mines are cause for public health concern because they are known sources of deleterious environmental metals such as uranium, lead, cadmium, and arsenic (Lewis et al. 2017). There are more than 4,000 abandoned uranium mines (AUMs) in the western United States, many of which are co-located with indigenous communities (Lewis et al. 2017) – including 523 AUMs on the Navajo Nation (NN). Despite evidence of links between exposure to metals found in AUM waste and human health impacts (Gonzales et al. 2018), there remains limited scholarship specifically addressing environmental exposure to metals among rural and underserved communities in the southwest United States.

Existing biomedical and environmental epidemiology investigations with indigenous communities have identified associations between environmental metals found in AUM waste and negative health outcomes (Erdei et al. 2019; Hund et al. 2015). Residential proximity to AUMs was associated with biological markers of cardiovascular disease (Harmon et al. 2018). Oral intake of uranium via drinking water has also been associated with immune system changes among NN residents (Erdei et al. 2019). While there are numerous investigations of human health and metal exposure in the southwest US, most include only limited exposure assessments (Gonzales et al. 2018) and few consider multiple routes of exposure.

On the NN there are multiple routes of potential metals exposure including inhalation via windblown dust (Beamer et al. 2014) and ingestion via drinking water or food items (deLemos et al. 2009; Hoover et al. 2019). Recent literature has suggested that air/dust might be a primary contributor to exposure. Indoor residential dust in Shiprock, New Mexico, a community in the Northern Agency of NN, indicated an abundance of uranium, cadmium, and lead. The metal mixtures present in dust collected from these homes were chemically similar to nearby AUM waste (Gonzalez–Maddux et al. 2014). Analysis of AUM waste in Blue Gap, Arizona, a community in the Central Agency of NN, contained uranium-bearing nanostructures small enough to be inhaled deeply into the lung (Zychowski et al. 2018). Aeolian (windblown) transport of metals from AUM sites may be particularly important for the NN because approximately one-third of the NN on the Colorado Plateau is covered with Aeolian sand (Bogle et al. 2015). Both environmental and anthropogenic soil disturbance may increase transport of dust containing metals from mining sites. The NN's complex terrain also plays a critical role in shaping how contaminants are transported from mine sites via air (Lindsey et al. 1999). While these studies demonstrate the potential for

environmental accumulation and movement of metals in air or water, there remains limited investigation of aggregated exposure potential from multiple pathways. This research directly addresses this literature gap.

Integration of inhalation and ingestion pathways (e.g., water, air, and soil) are therefore necessary to better estimate exposure potential. However, existing methods on contaminant fate and transport or physical process models are usually based on single pathways and require sophisticated environmental data that are rarely available in rural and Tribal areas (Lewis et al. 2017). For example, the American Mine Services/US Environmental Protection Agency (AMS/EPA) Regulatory Model (AERMOD) is the preferred method for modeling movement of particulate matter over large areas (within 50 kilometers of pollution sources); however, this method requires detailed emission source parameters such as pollutant emission rates and release height, detailed meteorological data, as well as background concentration levels. On the NN there are few monitoring stations to cover a land area of 70,000 km^2. Available emission source, environmental, and meteorological data are therefore insufficient for many sophisticated dispersion models. The use of more complex physical process models is therefore untenable, but the need for more detailed exposure potential spatial products remains. Consequently, there is very limited environmental modeling of contamination for AUM sites and surrounding areas.

To address this issue, this study employed existing and widely accepted geospatial and computational methods that to date have not been employed in the domain of AUM contamination potential on the NN. To wit: we leverage a GIS-based multi-criteria decision analysis (GIS-MCDA) approach based on available environmental information from multiple sources to address the public health need to map potential AUM waste exposure from multiple pathways across the NN as a large geographic area. The GIS-MCDA approach can relate known and observable effects of multiple exposure routes from pollution sources to the neighboring landscape and therefore is a common approach for risk mapping or vulnerability assessments. GIS-MCDA is a process that transforms and combines geospatial data and decision-maker's value judgments to obtain information for decision making (Malczewski 2006a). The method aggregates coincident criteria into one map representing a composite variable (Jiang & Eastman 2000; Malczewski 2006a) and has been used extensively for remedial site evaluations (Chen et al. 2019; Li et al. 2018), land use suitability (Chang et al. 2008; Charabi & Gastli 2011; Chen et al. 2010), risk mapping or vulnerability assessments (González Del Campo 2015; Hou et al. 2017; Rangel-Buitrago & Anfuso 2015), and public health studies (Young et al. 2010). Many studies have been conducted to integrate the GIS-MCDA models and fuzzy set theory to address potential uncertainties in the MCDA approach (Kuo et al. 2002), GIS-MCDA creates a product that can help evaluate risk or vulnerability level of contamination quantitatively and ranks/prioritizes geographic areas for further investigation. Spatial products generated using this approach may identify areas with greater potential for contamination, such as those within the NN where contamination risk from AUMs is the product of multiple environmental processes. This study is entirely a novel application and a crucial first step toward informing future epidemiologic studies and ongoing remediation efforts to reduce human exposure to AUM waste. For the purposes of this paper we adopt a description of risk mapping provided

by Lahr and Kooistra (2010) as the mapping and identification of areas that are vulnerable to contamination.

The objectives of this study were: 1) to develop a site-specific model for potential environmental risk mapping in the NN; 2) to conduct a sensitivity analysis of the model; and 3) to validate the model using a separate environmental dataset. This work provides the first detailed environmental risk map emphasizing combined pathways for AUM contamination on the NN using geospatial modeling and computational methods. Development of environmental risk maps for this region may inform future epidemiologic analysis, remediation decision making, and intervention research aimed to reduce exposure and improve human health. The framework illustrated in this paper could be extended to other research on geographic regions facing environmental issues to refine knowledge of complex contamination potential.

Material and methods

Study area

The study area is limited to the conterminous boundary of the Navajo Nation (NN), a sovereign indigenous nation located in the southwest United States. The NN is approximately 70,000 km^2 located in Arizona, New Mexico, and Utah and is divided into five administrative units (agencies): Eastern, Central, Northern, Western, and Ft. Defiance (Figure 1). The tribal lands of the NN are sparsely populated, with a large proportion of the population living in rural and geographically remote locations with limited infrastructure. The majority of the NN is located on the Colorado Plateau, with elevation ranging from 940–3,153 meters. More than half of the land area has an arid or desert climate. The population of the NN was 175,005 people in 2017, 95.3% of whom self-identified as indigenous. Economically, 52.3% of individuals living on the NN are unemployed and 40.4% of households have an annual income of less than $25,000 (U.S. Census Bureau n.d.).

Methodology

This study adopted a GIS-MCDA approach that used fuzzy logic to model potential for contamination from AUMs on the NN. The accumulative contamination potential was determined using a weighted linear combination (WLC) of eight standardized factors as a proxy of interaction with contamination pathways from AUMs. These pathways were modeled across a geographic surface representing specific spatial characteristics. The factors selected for risk analysis are:

- Proximity to AUM sites
- Proximity to roads
- Proximity to downslope drainages from AUM sites
- Topographic landforms
- Wind index
- Topographic wind exposure (TWE)

- Vegetation robustness (NDVI)
- Groundwater contamination

These factors were selected as they play a major role in the fate and transport of contaminants in the environment via different pathways. Detailed justification of each factor is discussed in the data preprocessing section. Proximity to AUMs, roads, and downslope drainage were modeled as the three primary risk factors. Topographic features, specifically valleys and lower slopes, represent a high likelihood of pollutant accumulation. Aeolian transport of dust was modeled as both TWE and a wind index, both of which consider areal location in relation to prevailing monthly winds. Finally, groundwater contamination interpolated from extant samples was used to account for the interaction between surficial contamination and transport below the pedosphere. Each factor was standardized using fuzzy membership. Factor weights were determined using pairwise comparisons in the analytic hierarchy process (AHP). Finally, the factors were aggregated and risk scores were generated using a WLC method. The overall framework of this paper is illustrated in Figure 2. The framework follows a standard workflow of GIS-MCDA approach (Hamzeh, Abbaspour, & Davalou 2015; Koshand et al., 2018) along with sensitivity analysis and model validation. We used fuzzy logic to standardize each factor layer and to mitigate uncertainties in risk mapping, which is not commonly seen in most traditional GIS-MCDA approaches.

Geographical data sets consisting of point locations for each AUM feature as well as surface and underground polygons of AUMs, of which there are 523 sites within the study area, were obtained from US Environmental Protection Agency (USEPA) (USEPA 2006). Wind data (daily wind direction over the past 30 years) from 14 regional and major airports (Figure 1) around the NN were obtained from historical meteorological aerodrome reports (METARs) (Iowa State University, n.d.). Topographic data, including landform classification, slope, and aspect, were generated using a digital elevation model (DEM) at 30-meter resolution obtained from the US Geologic Survey (USGS) (U.S. Geological Survey, n.d.). A road network was obtained as TIGER/line shapefiles from the U.S. Census Bureau (U.S. Census Bureau, n.d.). Downslope drainage area and groundwater quality data were obtained from USEPA (USEPA 2006) and an existing database at the University of New Mexico (Hoover et al. 2017), respectively. Vegetation data (normalized difference vegetation index [NDVI]) were obtained from the NASA Vegetation Index and Phenology (VIP) global dataset (Didan 2010). Scenes for every month between January 1984 and December 2014 were collected and averaged into monthly datasets.

Data preprocessing

Proximity to Abandoned Uranium Mines—Proximity to contamination sources plays a critical role in contaminant transport and dispersion. Numerous studies have used proximity as a proxy for contamination or exposure (Gong et al. 2016). Previous studies on AUMs on the NN found that residential proximity to AUMs was associated with elevated arsenic and uranium concentration in the environment and adverse health outcomes (deLemos et al. 2009; Hoover et al. 2017; Harmon et al. 2017).

In this study, proximity to AUMs was calculated as the square root of the sum of the inverse distances of a geographic location to all AUM features within 50 kilometers, and weighted by the surface area of each feature (adapted from Harmon et al (2017)):

$$P_i = \sqrt{\sum_{j=1}^{m} \frac{w_j}{D_{ij}}} \quad for\left(D_{ij} \leq 50km\right) \tag{1}$$

$$w_j = \widehat{wJ} \Big/ \sum_{k=1}^{N} \widehat{wk}, \ \widehat{wJ} = \sqrt{areaj}$$

where P_i is AUM proximity score, I is the spatial location of the centroid of interest, j is any AUM within a 50 kilometer threshold of I, m is the number of AUMs within the threshold, and w_j is a weight based on the proportion of the size of the nearest AUM and all others within the threshold.

Due to the fact that proximity alone does not fully explain measured contamination in the environment or biomonitoring data in previous studies on the NN (Erdei et al. 2019; Lewis et al. 2017), the following factors were included in the model based on their role in contaminants fate and transport.

Proximity to Roads—Roads are considered a pathway of heavy metal contaminants and pollutant dispersion from AUMs, largely due to dust associated with traffic, both on paved and unpaved roads (Apeagyei et al. 2011; Duong & Lee 2011). The inclusion of this factor was based on the EPA's NN AUM Screening Assessment Report (EPA 2007) which found increased concentration in contaminants with increased proximity to roads. Proximity to roads was calculated as the Euclidean distance from each road segment.

Proximity to Downslope Drainage—Pollutants from AUMs may be transported via surface water in ephemeral or perennial drainages. Previous research shows that environmental media in drainages downstream of AUMs contain metals found in AUM waste largely because of high water solubility of contaminants (deLemos et al. 2009; Lameman Austin 2012). The EPA's NN AUM Screening Assessment Report (EPA 2007) also found increased concentration in contaminants with increased proximity to downslope drainage. The proximity to these drainages was calculated as the Euclidean distance from each drainage.

Landform Classification—Much of the physical geography of the NN is typified with flat or gentle slopes incised with steep, precipitous valleys and lower slopes. These lower regions receive downhill air flow wherein winds may be naturally directed – transporting metals from AUM sites (Deacon 1969). Different landforms have been identified as an important factor in pollutant dispersion in several physical process models that consider air and soil pathways (Yudego et al. 2018). Landforms were identified across the study area by first calculating the topographic position index (TPI) (Jenness 2006) from elevation values in a 30-meter DEM. TPI is a dimensionless value that is determined by comparing the pixel of interest with the elevations of pixels in a user-specified neighborhood. Using a 5-pixel

neighborhood, 6 landforms were identified based on TPI: valleys, steep slopes, gentle slopes, lower slopes, ridges, and flat land. A detailed procedure of how each landform is classified can be found elsewhere (Jenness 2006). All parameters in the landform classification were calibrated with an accuracy assessment through random sampling as discussed in the results section.

Wind Index—Wind in the NN is both culturally-significant (McNeley 1981; Sherry 2002) and a prevalent feature of the physical landscape. Recent warming trends and historic land use patterns have led to an increase in Aeolian sediment mobility characterized by large sand dune migration and substantial dust storms (Draut et al. 2012). Most air dispersion models consider wind direction relative to contamination sources (e.g. leeward and windward) (Elangasinghe et al. 2015; Kim et al. 2015). As such, a wind index is used to model general patterns of wind-borne fugitive dust from AUMs across the study area. The wind index is a scaled value between 0 and 1 calculated based on the equation (Ryan et al. 2008):

$$Wind\ Index = \frac{1 - \cos(\theta - \beta)}{2} \quad (2)$$

where θ is the Euclidean direction from the nearest AUM and β is the prevailing wind direction of any geographic location in the study area in degrees. Locations directly downwind of the nearest AUM have a wind index value of 1, those perpendicular to the wind direction have an index of 0.5, and those upwind have an index near 0.

Prevailing wind direction was obtained based on wind rose plots of 30-year wind information measured weekly at 14 regional and major airports in and around the NN for each month (Figure 1). Each pixel in the study area was assigned the monthly prevailing wind value of the nearest airport. A wind index was generated for each month using monthly wind direction.

Topographic Wind Exposure—Existing models acknowledge the effect of topographic terrain on Aeolian transport (Yudego et al. 2018). Therefore, we used the topographic wind exposure (TWE) to model localized vulnerability of dust exposure by relating the angle of wind incidence to physical features. Studies have demonstrated the validity of TWE in predicting contaminant dispersion (Böhner & Antonić 2009). TWE is a calculation of the angle between a plane orthogonal to the wind and a plane that represents the local topography according to the equation (Antonić & Legović 1999; Böhner & Antonić 2009):

$$\cos\alpha = \cos(\mu)\sin(\beta) + \sin(\mu)\cos(\beta)\cos(\delta - \gamma) \quad (3)$$

where $\cos\alpha$ is the angle of TWE, μ is the terrain slope calculated from a DEM, β is the horizontal angle of wind, δ is the wind direction, and γ is the terrain aspect also calculated from a DEM. For the scope of this study, only wind horizontal to flat ground was considered ($\beta = 0$). Topographic wind exposure was derived for each month due to the monthly variation in wind direction.

Groundwater Contamination—About 30% of NN residents rely on unregulated water sources, including groundwater wells (deLemos et al. 2009). The hydrogeology of the region

includes 3 primary aquifer units, each comprised of multiple water bearing formations (Cooley et al. 1969). To account for potential exposure to metals via groundwater we calculated a hazard index (HI) score for 467 groundwater sources across the NN previously tested for arsenic and uranium concentrations (Hoover et al. 2018) and interpolated the results as a proxy measure of potential contamination, informed by existing water quality results (Gong et al. 2014). Previous research on the NN demonstrated a spatial clustering of elevated arsenic and uranium in groundwater sources proximal to AUM sites (Hoover et al. 2017).

Vegetative Robustness—Vegetation cover and substrate reduces the transport of windblown dust (Bogle et al. 2015; Draut et al. 2012). Existing physical models such as DUSTRAN (A GIS-Based Atmospheric Dust Dispersion Modeling System) model Aeolian transport using vegetation cover as a significant factor (Allwine et al. 2006). Largely, the NN is sparsely vegetated and is typified by low scrub and brush (Draut et al. 2012). Forested areas in Navajo land extend from the southeastern up to the north-central portions. Monthly 30-year averages of normalized difference vegetation index (NDVI) were calculated to capture the broad trends of vegetative phenology across the study area in order to predict the likelihood of impeding windblown dust transport. The NDVI values range between −1 and 1. Values approaching 1 indicate the highest level of vegetative cover and thus low likelihood of facilitating windblown dust transport and those of 0 and smaller indicate bare earth and thus high likelihood of facilitating windblown dust transport.

All above environmental factors were preprocessed and mapped in a GIS software – ESRI ArcMap 10.4.1.

Fuzzy membership

Each of the criteria layers were standardized using the fuzzy logic technique, which has been widely used to address uncertainties in environmental risk assessment processes (Eldrandaly 2013). Fuzzy membership values range from 0 to 1 and indicate the degree to which an input value represents the set as a whole (ESRI 2016; Zadeh 1965). Four algorithms were used to transform input raster values to fuzzy membership values, using ESRI ArcMap (v. 10.4). The fuzzy large (monotonically increasing sigmoidal) function indicates that larger values in the input dataset have a higher degree of membership and therefore present a higher potential for contamination. Fuzzy small (monotonically decreasing sigmoidal) is the inverse of fuzzy large wherein larger input values indicate lower membership (lower risk of contamination). The fuzzy MS large algorithm is similar to fuzzy large, but the midpoint and spread are defined by the mean and standard deviations of input raw values. The fuzzy MS small algorithm is the inverse of MS large.

Fuzzy functions were selected based on the following assumptions for each factor layer. Areas with higher AUM proximity, wind index, TWE, or groundwater hazard index have greater potential for AUM contamination; conversely, areas with low vegetation index values have greater contamination potential due to soil instability and windblown dust. Areas close to roads and drainages downstream of AUMs may also have higher contamination potential.

Lastly, valleys and lower slopes were considered to be associated with higher vulnerability to contamination risk due to the greater likelihood of pollutant accumulation (Deacon 1969).

Analytic hierarchy process

A pairwise comparison among the factors following the AHP method was completed to determine weights for each factor. The pairwise rank between two factors was assigned based on literature (Bogle et al. 2015; deLemos et al. 2009; Hoover et al. 2017; Lindsey et al. 1999; Lowe et al. 2018), the research team's knowledge of the study area through in-person field work, and conversations with experts and local residents. The priority ranks satisfy the additivity constraint (Chen et al. 2010; Saaty 1977), where the sum of all weights equal 1.

Factors were aggregated using the WLC method based on the generated weights according to the following equation (Malczewski 2006b):

$$r_i = \sum_{j=1}^{n} w_j a_{ij} \tag{4}$$

where r_i is the risk value at location i, w_j is the criterion weight, and a is the criterion value at location i for criterion j.

Specifically, a weighted sum was applied for each standardized factor layer and the aggregation was conducted for each month. The overall estimated environmental risk score of contamination ranges between 0 and 1, representing lowest to highest risk, respectively.

Sensitivity analysis and model validation

In order to ascertain the degree to which the input factor weights influence the model, a sensitivity analysis using the one-at-a-time (OAT) method was conducted where each weight was incrementally adjusted by a percent change (PC) for a range of percent change (RPC) of ±20% and reapplied to the weighted linear combination. Following Chen and colleagues (2010), when each individual weight is adjusted, the associated weights of the other criteria layers must be moderately adjusted to ensure that the additivity constraint is consistently met. This process was implemented using Python scripting in the arcpy environment and the following equation:

$$W(c_i, pc) = (1 - W(c_m, pc)) \times \frac{W(c_i, 0)}{(1 - W(c_m, 0))}, i \neq m, 1 \leq i \leq n \tag{5}$$

where $W(c_i, pc)$ is the weight of the i^{th} criterion, c_i at the base run, c_m is the main changing criterion, and n equals the total number of criteria in the model.

A total of 320 results were generated for each one-month period employing the OAT method (Chen et al. 2010; Daniel 1973). Change was quantified in terms of how many pixels in the results fell within low (R1), medium (R2), or high (R3) risk groups, defined as tertiles of the initial overlay (0 PC). To reduce the computational burden, only surfaces for April and September were analyzed in the sensitivity analysis, as they are representative of high and low windy seasons and vegetation tends to be at different phenological stages. It should be

noted that the differences in wind characteristics might not be captured due to a lack of wind speed data used in the study.

The environmental risk scores were validated using uranium concentrations in sediment and soil samples collected across the NN as part of the National Uranium Resource Evaluation (NURE) Hydrogeochemical and Stream Sediment Reconnaissance dataset (U.S. Geological Survey 1975) as well as EPA's Airborne Spectral Photometric Environmental Collection Technology (ASPECT) data of detected radiation levels (USEPA 2019). Because both datasets are spatially autocorrelated, meaning they exhibit nonstationary relationships (p-value for Moran's I tests on both datasets < 0.001), a geographically weighted regression (GWR) was applied to test the statistical fit between ground data and the modeled risk score. GWR is a local form of linear regression which has been widely used to model spatially varying relationships (Fotheringham et al. 2002).

Results

Environmental factors

Figure 3 presents individual factor surface results for the month of April. Results indicated areas in Eastern, Northern, and Western Agencies with higher AUM proximity values due to the concentration of AUM sites in these areas (Figure 3a). Drainage areas located downslope of AUMs followed a similar pattern with the highest downstream distances located the furthest from areas with high AUM proximity values (Figure 3c). The groundwater contamination map (Figure 3h) also followed this general pattern but an area of elevated contamination was observed in the Ft. Defiance agency away from AUM locations. The wind index map (Figure 3g) is centered on AUMs and is reflective of prevailing wind direction observations in sub-regions. The TWE map illustrates a positive index value for terrain features with aspects coincident to prevailing monthly winds (Figure 3f).

Landform classification results indicated that 65% of the study area was classified as gentle slopes, 20% as upper slopes, 12% lower slopes, 2% ridges, 0.18% valleys below steep slopes, and 0.05% steep slopes (Figure 3d). The landform classification accuracy assessment indicated that 86% of the landforms were correctly classified using the specified model.

The vegetation index map (Figure 3e) illustrated higher values in the central forested areas proximal to the New Mexico/Arizona border and lower index values in eastern and southwestern NN where barren land is common. Additionally, the proximity to roads map (Figure 3b) suggests a fairly dense road network through the NN with small patches of lower road density and a limited number of roads in an area in the northwestern NN along the Colorado River and Grand Canyon National Park.

Initial modeled results

In total, 41 fuzzy surfaces were generated including monthly models for vegetation cover, topographic wind exposure, and the wind index. A single fuzzy surface was created for the other 5 factors that are not temporally variable. Descriptive statistics for the fuzzy layers, where a membership value close to 1 indicates greater contamination risk, are presented in Table 2.

Factor weights were determined based on AHP input. From 28 comparisons in the AHP process, a consistency ratio (CR) of 9.4% was reached with a principal eigenvalue of 8.921. The resultant decision matrix and output factor weights are presented in Table 3. There is minimal quantitative difference between the overlay results for all 12 months. Monthly results are listed in the supplemental document table S1.

Figure 4 shows a risk surface generated as an average of the 12 monthly surfaces. There are three areas of higher contamination potential that align with the proximity to AUMs, due to the high weight assigned to this factor. Within these areas, potential contamination varies based on other factors. The northwestern corner of the Western Agency along the Colorado River, northeastern corner of Eastern Agency, as well as several areas in the south-central area of Ft. Defiance Agency have relatively low risk values because these areas are further from AUMs, roads, or drainages, which were the top three weighted factors. Because fuzzy values are dimensionless, the degree of risk represented in the overlay models is relative to all pixels contained within the study area limits.

Sensitivity analysis and model validation results

The initial sensitivity test focused on results for the month of April (typically windy season), which was compared to September (typically non-windy season). If incremental adjustment of input weights affects little to no change in the output overlay results, the model is insensitive to minor changes and demonstrates good overall strength. Three risk groups (low (R1), medium (R2), and high (R3)) were defined using the following intervals: 0.139 – 0.399, 0.399 – 0.659, and 0.659 – 0.918.

Figure 5 shows the sensitivity analysis results from 320 simulations for each factor in the month of April. Amongst all factors, the majority of the study area was dominated by the medium risk classification (R2). Having the highest weight in the model, proximity to AUMs and proximity to roads demonstrated a moderate degree of sensitivity, while the remaining six factors were relatively stable. For proximity to AUMs, significant change started at the +8 PC in weights where the low risk (R1) areas grow and medium risk (R2) as well as high risk (R3) areas shrink. For proximity to roads, the low risk (R1) areas decreased while the medium risk (R2) and high risk (R3) areas increased, with the most salient change observed below −14 PC in weights. While the drainage and landform factors were relatively stable, the conceptualizations of low risk (R1) and high risk (R3) approached convergence near the lower and upper extremes of the sensitivity analysis, respectively. The sensitivity analysis results were similar for the month of September (see supplementary file table S2).

The adjusted weight values and pixel counts per risk grouping at each PC using the proximity to AUMs in April and September as an example are presented in supplement file table S2. For both months, the average change of the number of cells in low, medium, and high risk groups was 3%, −0.6%, and −0.9%, respectively, for every 1% change in the weight of proximity to AUMs. The average change imparted on the overlay maps when adjusting weight values for all other criteria maps was less pronounced, with a less than 1% change in tertile membership for every simulation run.

In order to better visualize the sensitivity spatially, we calculated the standard deviations of risk scores across the study area surface from all 320 test runs for April (Figure 6). We observed a low standard deviation (low sensitivity) in the three clusters of high risk areas in close proximity to AUMs.

The R^2 of GWR for each monthly contamination risk score are presented in Table 4. The average R^2 is 0.84 using ASPECT data and 0.95 using NURE data across all months, suggesting a strong fit between modeled results and environmental monitoring data.

Discussion

This study created a GIS-MCDA model for environmental risk mapping to identify areas at greatest vulnerability to contamination from AUM sites on the NN. The model accounts for proximity to AUMs, meteorology, topography, vegetation, and proximity to roads and surface drainages. To date, no studies have included this combination of environmental factors for mapping potential AUM contamination for the full spatial extent of the NN. This approach is a viable assessment method for modeling contamination potential in the absence of comprehensive environmental and metrological monitoring across the study area.

Based on the results of this study, 20.2% of NN are at higher risk (R3) for AUM contamination, and 65.7% and 14.1% areas are at medium (R2) and lower risk (R1), respectively. Three areas with higher risk are observed close to AUMs, due to the higher relative weight for AUM proximity (above 40%). Elevated home dust metal concentration as well as water contamination of arsenic and uranium has been found in areas close to AUM sites in the NN (deLemos et al. 2009; Gonzalez–Maddux et al. 2014; Hoover et al. 2017). Residents of Navajo communities who self-reported exposure to AUM tailings in the Eastern Agency (New Mexico portion of NN, see Figure 1) demonstrated an elevated risk for diabetes, hypertension, and kidney disease (Hund et al. 2015). Additionally, serum inflammatory markers from 273 Navajo men and women living in the Eastern Agency were inversely associated with residential proximity to abandoned waste piles and induction of a pathway leading to development of atherosclerosis and cardiovascular disease (Harmon et al. 2017). In this area of the NN, our team also identified that living close to AUM sites and U contamination in the drinking water increased the risk of developing environmentally induced autoimmune biomarkers, potentially increasing the risk of the development of severe immune dysfunction (Erdei et al. 2019).

Although the environmental risk map is most influenced by proximity to AUMs, proximity to roads, drainages, and landforms (valleys and lower slopes) also influenced the aggregated output. Road dust contamination has been well documented in mining areas (Yang et al. 2016) and is likely a source of airborne dust in the study area because the majority of the roads in the NN are unpaved (>83%). Moreover, an association between exposure to road dust and high rates of asthma prevalence and severity among Navajo children exists (Lowe et al. 2018). Contaminants from AUMs and roads may be dispersed by winds. This process is impacted by wind direction, wind speed, vegetation cover, and terrain factors, which were quantified in terms of the wind index, topographic wind exposure, vegetation index, and a landform classification. Although these factors account for a small portion of the overall

weight (16%), their role has been well documented in the literature (Bogle et al. 2015; Lindsey et al. 1999).

This study also considered drainages downstream of AUMs as potential water pathways for contamination because they transport contaminants during episodic flooding (Lameman Austin 2012). Some contaminants, such as uranium from AUMs, are highly soluble and thus water concentration is much higher for those contaminants when they are saturated with rainwater (deLemos et al. 2009). As such, we included the proximity to downstream drainages since the surficial contaminants can be leached and accumulated in the adjacent soils. Groundwater resources in surficial alluvium may be contaminated by run off from AUM sites, as has been documented along the Rio Puerco in Eastern Agency (deLemos et al. 2009; Rock 2017). Groundwater concentrations of arsenic and uranium may also be elevated in deeper aquifers because the uranium bearing formations are the same water bearing formations that residents may use for livestock watering (Hoover et al. 2017).

In this study, we used a WLC to model the interaction between factors standardized with fuzzy membership. Many environmental service or risk models employ linear aggregation methods (Gemitzi et al. 2006) largely because, while certain ecological processes will result in repercussions across space, they do not entirely supplant other processes. In other words, factors in environmental models are usually present despite diminished relative influence on the observed phenomenon.

This study adopted a well-established workflow which first developed a fuzzy AHP, determined factors weights, and collected and processed data for decision making (Kuo et al. 2002). This workflow has been widely used in GIS-MCDA and remains relatively unchanged, though there has been considerable research into the specific methods employed therein. The most pronounced component to this workflow has emerged in the form of model validation and sensitivity assessments.

The validity of MCDA models is tested in a number of ways. Uncertainty and sensitivity may be quantified through techniques such as the Dempster-Shafer Theory (DST) to understand information representation and combination (Feizizadeh & Blaschke 2013). Monte Carlo simulation (MCS) is a similar technique where adjustments and inputs are statistically randomized, allowing for a higher degree of variability while minimizing computational burden (Chang et al. 2008; Paquette & Lowry 2012). This study adopted the one-at-a-time (OAT) method which incrementally adjusts criteria weights by set amounts in a highly controlled set of simulation runs (Chen et al. 2010; Daniel 1973; Eldrandaly 2013). The model in this study has been proven consistent based on sensitivity analysis.

Ground truth validation has also proven to be a viable measure of model reliability (Fuller et al. 2003). However, many models are limited in terms of availability of reliable data against which conclusions may be validated. The NURE samples used in the current study included soil (17%), stream sediment (81%), and spring sediment samples (2%) (n = 4344). We observed a strong fit between the NURE soil and sediment samples collected in the NN and our overall modeled results. Further examination of GWR residuals revealed that the overall model with the 8 factors significantly improved the final modeled results which produced

randomly distributed residuals compared with the proximity-based model that only used the proximity factor as the environmental contamination potential which had a poor fit in geographic areas close to AUMs.

Limitations

This study has several limitations. First, it is critical to select control points of fuzzy membership functions. The middle point of the fuzzy membership functions was set to the numeric mean value of the inputs such that the maximum fuzzy value of the membership of any criterion is equal to half of all of the instances of any other fuzzy value in the set (Yen & Langari 1999).

This set compliment holds that nothing is certainly known about the distribution of observable phenomena represented in the set and, by extension, the interaction between criteria within the model. Future work should conduct a rigorous sensitivity analysis on the choice of different control points of fuzzy membership functions.

Second, although we adopted AHP to derive factor weights, subjectivity still exists in factor ranking and thus derived weights. Existing work has conducted uncertainty analysis on AHP factor rank and associated results (Feizizadeh & Blaschke 2013). The current study conducted rigorous sensitivity analysis and found that the model is not sensitive to the majority of the factors. Future work should consider uncertainty analysis as well.

Third, wind speed was not used in the model, which might impact the air/dust flow in the study. The seasonal variation (e.g. windy season vs non-windy season) was not truly reflected in the study due to the ignorance of wind speed, which possibly explains the relatively minor differences among monthly overlay results. However, the factors (e.g., wind index and topographic wind exposure) do not have wind speed built in the function. Future work should include wind speed in the wind index or topographic wind exposure factors. Furthermore, wind data at finer spatial scales should be used when available. Wind data from the North American Regional Reanalysis at 32 km grid should be considered in future work. Fourth, the Hopi Reservation, which is encompassed by the NN, was not included in the risk analysis due to incongruent environmental information available within its boundary. Two coal mine sites across the NN and Hopi, Black Mesa and Kayenta mines, should be included if research focuses on contamination in general.

Lastly, as discussed above, this study was limited by the availability of detailed datasets with which sophisticated models may be constructed or validated. Existing air quality dispersion models (e.g., AERMOD, CALINE3, and CTDMPLUS) provide more accurate estimates. However, our current study could not adopt these models due to a lack of detailed emission source data and the large footprint of the study area. Regardless, this study aimed to estimate the relative risk or vulnerability level rather than absolute contaminants concentration in the environment. Thus, the use of GIS-MCDA is sufficient in addressing this question. Also, the NURE and ASPECT datasets are pure environmental datasets which might not capture all of the contamination pathways. Future work should collect a variety of more contemporary environmental samples (air, dust, water, and soil) to test the validity of the model.

Meanwhile, future work should consider using biomonitoring data as another source for validation.

Conclusion

This is the first study to use a GIS-MCDA framework to map potential for abandoned uranium mine contamination on the NN. We considered multiple contamination pathways including air and water transport of contamination from AUM sites. The model was tested with a rigorous sensitivity analysis and ground truth validation. The results of this modeling work indicated that 20.2% of the NN was at higher risk for AUM contamination, specifically areas of Eastern, Northern, and Western Agencies due to the proximity to AUM sites. Several areas far from AUM sites also demonstrated elevated contamination potential when different environmental processes were considered. The sensitivity analysis and validation work demonstrated the reliability of the model in the study. This work provides novel modeling information illustrating areas of higher potential contamination by combining AUM locations with roads, drainages, meteorological factors, topographic factors, as well as other physical characteristics. Although further model refinement and validation using other environmental data is suggested, this research may prove useful to tribal, state, and federal agencies working to remediate abandoned uranium mines and reduce human exposure to harmful contaminants found in these wastes.

Supplementary Material

Refer to Web version on PubMed Central for supplementary material.

Acknowledgements

This work was supported by National Institutes of Health grants 1P50ES026102 and 1P42ES025589, and Assistance Agreement No. 83615701 awarded by the U.S. Environmental Protection Agency to the University of New Mexico Health Sciences Center. This work has not been formally reviewed by US EPA or NIH. The views expressed are solely those of the authors and do not necessarily reflect those of these Agencies.

References

Allwine KJ, Rutz FC, Shaw WJ, Rishel JP, Fritz BG, Chapman EG, … & Seiple TE (2006). DUSTRAN 1.0 User's Guide: A GIS-Based Atmospheric Dust Dispersion Modeling System (No. PNNL-16055). Pacific Northwest National Lab.(PNNL), Richland, WA (United States).

Antonić O, & Legović T (1999). Estimating the direction of an unknown air pollution source using a digital elevation model and a sample of deposition. Ecological Modelling, 124(1), 85–95. 10.1016/S0304-3800(99)00149-0

Apeagyei E, Bank MS, & Spengler JD (2011). Distribution of heavy metals in road dust along an urban-rural gradient in Massachusetts. Atmospheric Environment, 45(13), 2310–2323. 10.1016/j.atmosenv.2010.11.015

Beamer PI, Sugeng AJ, Kelly MD, Lothrop N, Klimecki W, Wilkinson ST, & Loh M (2014). Use of dust fall filters as passive samplers for metal concentrations in air for communities near contaminated mine tailings. Environmental Science: Processes & Impacts, 16(6), 1275–1281. 10.1039/C3EM00626C [PubMed: 24469149]

Bogle R, Redsteer MH, & Vogel J (2015). Field measurement and analysis of climatic factors affecting dune mobility near Grand Falls on the Navajo Nation, southwestern United States. Geomorphology, 228, 41–51. 10.1016/j.geomorph.2014.08.023

Böhner J, & Antonić O (2009). Chapter 8 Land-Surface Parameters Specific to Topo-Climatology. In Hengl T & Reuter HI (Eds.), Developments in Soil Science (pp. 195–226). 10.1016/S0166-2481(08)00008-1

Chang N-B, Parvathinathan G, & Breeden JB (2008). Combining GIS with fuzzy multicriteria decision-making for landfill siting in a fast-growing urban region. Journal of Environmental Management, 87(1), 139–153. 10.1016/j.jenvman.2007.01.011 [PubMed: 17363133]

Charabi Y, & Gastli A (2011). PV site suitability analysis using GIS-based spatial fuzzy multi-criteria evaluation. Renewable Energy, 36(9), 2554–2561. 10.1016/j.renene.2010.10.037

Chen R, Xiong Y, Li J, Teng Y, Chen H, & Yang J (2019). Comparison of multi-criteria analysis methodologies for the prioritization of arsenic-contaminated sites in the southwest of China. Environmental Science and Pollution Research, 26(12), 11781–11792. 10.1007/s11356-019-04642-z [PubMed: 30815813]

Chen Y, Yu J, & Khan S (2010). Spatial sensitivity analysis of multi-criteria weights in GIS-based land suitability evaluation. Environmental Modelling & Software, 25(12), 1582–1591. 10.1016/j.envsoft.2010.06.001

Cooley ME, Harshbarger JW, Akers JP, Hardt WF, & Hicks ON (1969). Regional hydrogeology of the Navajo and Hopi Indian reservations, Arizona, New Mexico, and Utah, with a section on vegetation (No. 521-A). US Government Printing Office.

Daniel C (1973). One-at-a-Time Plans. Journal of the American Statistical Association, 68(342), 353–360. 10.1080/01621459.1973.10482433

Deacon EL (1969). Physical processes near the surface of the earth. Retrieved from https://publications.csiro.au/rpr/pub?list=BRO&pid=procite:d4fb75fd-fcbf-4406-9803-f0fe5cb7966e

deLemos JL, Brugge D, Cajero M, Downs M, Durant JL, George CM, … Lewis J (2009). Development of risk maps to minimize uranium exposures in the Navajo Churchrock mining district. Environmental Health, 8(1), 29 10.1186/1476-069X-8-29 [PubMed: 19589163]

Didan K (2010, 7). Multi-satellite earth science data record for studying global vegetation trends and changes. In Proceedings of the 2010 international geoscience and remote sensing symposium, Honolulu, HI, USA (Vol. 2530, p. 2530).

Draut AE, Redsteer MH, & Amoroso L (2012). Vegetation, Substrate, and Eolian Sediment Transport at Teesto Wash, Navajo Nation, 2009–2012 (No. Scientific Investigations Report 2012–5095). U.S. Geological Survey.

Duong TTT, & Lee B-K (2011). Determining contamination level of heavy metals in road dust from busy traffic areas with different characteristics. Journal of Environmental Management, 92(3), 554–562. 10.1016/j.jenvman.2010.09.010 [PubMed: 20937547]

Elangasinghe MA, Dirks KN, Singhal N, Salmond JA, Longley I, & Dirks VI (2016). A simple tool to identify representative wind sites for air pollution modelling applications. Advances in Meteorology, 2016.

Eldrandaly KA (2013). Exploring multi-criteria decision strategies in GIS with linguistic quantifiers: An extension of the analytical network process using ordered weighted averaging operators. International Journal of Geographical Information Science, 27(12), 2455–2482. 10.1080/13658816.2013.815356

EPA. (2007). Abandoned Uranium Mines and the Navajo Nation Navajo Nation AUM Screening Assessment Report And Atlas With Geospatial Data. https://www.epa.gov/sites/production/files/2017-01/documents/navajo_nation_aum_screening_assess_report_atlas_geospatial_data-2007-08.pdf

EPA. (2019). EPA's Airborne Spectral Photometric Environmental Collection Technology (ASPECT). https://www.epa.gov/emergency-response/aspect

Erdei E, Shuey C, Pacheco B, Cajero M, Lewis J, & Rubin RL (2019). Elevated autoimmunity in residents living near abandoned uranium mine sites on the Navajo Nation. Journal of Autoimmunity, 99, 15–23. 10.1016/j.jaut.2019.01.006 [PubMed: 30878168]

ESRI. (2016). How Fuzzy Membership works—Help | ArcGIS for Desktop. Retrieved May 17, 2019, from http://desktop.arcgis.com/en/arcmap/10.3/tools/spatial-analyst-toolbox/how-fuzzy-membership-works.htm

Feizizadeh B, & Blaschke T (2013). GIS-multicriteria decision analysis for landslide susceptibility mapping: Comparing three methods for the Urmia lake basin, Iran. Natural Hazards, 65(3), 2105–2128. 10.1007/s11069-012-0463-3

Fotheringham AS, Brunsdon C, & Charlton M (2003). Geographically weighted regression: the analysis of spatially varying relationships. John Wiley & Sons.

Fuller DO, Williamson R, Jeffe M, & James D (2003). Multi-criteria evaluation of safety and risks along transportation corridors on the Hopi Reservation. Applied Geography, 23(2–3), 177–188. 10.1016/j.apgeog.2003.08.010

Gemitzi A, Petalas C, Tsihrintzis VA, & Pisinaras V (2006). Assessment of groundwater vulnerability to pollution: A combination of GIS, fuzzy logic and decision making techniques. Environmental Geology, 49(5), 653–673. 10.1007/s00254-005-0104-1

Gong G, Mattevada S, & O'Bryant SE (2014). Comparison of the accuracy of kriging and IDW interpolations in estimating groundwater arsenic concentrations in Texas. Environmental research, 130, 59–69. [PubMed: 24559533]

Gong X, Zhan FB, Brender JD, Langlois PH, & Lin Y (2016). Validity of the Emission Weighted Proximity Model in estimating air pollution exposure intensities in large geographic areas. Science of The Total Environment, 563, 478–485. [PubMed: 27152989]

Gonzales M, Erdei E, Hoover J, & Nash J (2018). A Review of Environmental Epidemiology Studies in Southwestern and Mountain West Rural Minority Populations. Current Epidemiology Reports, 5(2), 101–113. 10.1007/s40471-018-0146-z [PubMed: 30906685]

González Del Campo A (2015). GIS in Environmental Assessment: A Review of Current Issues and Future Needs. In Progress in Environmental Assessment Policy, and Management Theory and Practice (Vols. 1–0, pp. 121–143). 10.1142/9781783268382_0007

Gonzalez–Maddux C, Marcotte A, Upadhyay N, Herckes P, Williams Y, Haxel G, & Robinson M (2014). Elemental composition of PM2.5 in Shiprock, New Mexico, a rural community located near coal–burning power plants and abandoned uranium mine tailings sites. Atmospheric Pollution Research, 5(3), 511–519. 10.5094/APR.2014.060

Hamzeh M, Ali Abbaspour R, & Davalou R (2015). Raster-based outranking method: a new approach for municipal solid waste landfill (MSW) siting. Environmental Science and Pollution Research, 22(16), 12511–12524. 10.1007/s11356-015-4485-8 [PubMed: 25903176]

Harmon ME, Lewis J, Miller C, Hoover J, Ali A-MS, Shuey C, … Campen MJ (2017). Residential proximity to abandoned uranium mines and serum inflammatory potential in chronically exposed Navajo communities. Journal of Exposure Science and Environmental Epidemiology, 27(4), 365–371. 10.1038/jes.2016.79 [PubMed: 28120833]

Hoover J, Erdei E, Nash J, & Gonzales M (2019). A Review of Metal Exposure Studies Conducted in the Rural Southwestern and Mountain West Region of the United States. Current Epidemiology Reports, 6(1), 34–49. 10.1007/s40471-019-0182-3 [PubMed: 30906686]

Hoover J, Gonzales M, Shuey C, Barney Y, & Lewis J (2017). Elevated Arsenic and Uranium Concentrations in Unregulated Water Sources on the Navajo Nation, USA. Exposure and Health, 9(2), 113–124. 10.1007/s12403-016-0226-6 [PubMed: 28553666]

Hoover J, Coker E, Barney Y, Shuey C, & Lewis J (2018). Spatial clustering of metal and metalloid mixtures in unregulated water sources on the Navajo Nation – Arizona, New Mexico, and Utah, USA. Science of The Total Environment, 633, 1667–1678. 10.1016/j.scitotenv.2018.02.288 [PubMed: 29669690]

Hou D, O'Connor D, Nathanail P, Tian L, & Ma Y (2017). Integrated GIS and multivariate statistical analysis for regional scale assessment of heavy metal soil contamination: A critical review. Environmental Pollution, 231, 1188–1200. 10.1016/j.envpol.2017.07.021 [PubMed: 28939126]

Hund L, Bedrick EJ, Miller C, Huerta G, Nez T, Ramone S, … Lewis J (2015). A Bayesian framework for estimating disease risk due to exposure to uranium mine and mill waste on the Navajo Nation. Journal of the Royal Statistical Society: Series A (Statistics in Society), 178(4), 1069–1091. 10.1111/rssa.12099

Iowa State University. (n.d.). IEM: ASOS/AWOS Network. Retrieved June 20, 2019, from Iowa Environmental Mesonet of Iowa State University website: https://mesonet.agron.iastate.edu/ASOS/

Jenness J (2006). Topographic Position Index (TPI) v. 1.2 (No. 1.2). Retrieved from http://www.jennessent.com/downloads/tpi_documentation_online.pdf

Jiang H, & Eastman JR (2000). Application of fuzzy measures in multi-criteria evaluation in GIS. International Journal of Geographical Information Science, 14(2), 173–184. 10.1080/136588100240903

Khoshand A, Bafrani AH, Zahedipour M, Mirbagheri SA, & Ehtehsami M (2018). Prevention of landfill pollution by multicriteria spatial decision support systems (MC-SDSS): development, implementation, and case study. Environmental Science and Pollution Research, 25(9), 8415–8431. 10.1007/s11356-017-1099-3 [PubMed: 29307066]

Kim KH, Lee SB, Woo D, & Bae GN (2015). Influence of wind direction and speed on the transport of particle-bound PAHs in a roadway environment. Atmospheric Pollution Research, 6(6), 1024–1034.

Kuo RJ, Chi SC, & Kao SS (2002). A decision support system for selecting convenience store location through integration of fuzzy AHP and arti®cial neural network. Computers in Industry, 16.

Lahr J, & Kooistra L (2010). Environmental risk mapping of pollutants: state of the art and communication aspects. Science of the Total Environment, 408(18), 3899–3907. [PubMed: 19939435]

Lameman Austin TL (2012). Distribution of uranium and other trace constituents in drainages downstream from reclaimed uranium mines in Cove wash, Arizona (University of New Mexico). Retrieved from https://digitalrepository.unm.edu/wr_sp/91

Lewis J, Hoover J, & MacKenzie D (2017). Mining and Environmental Health Disparities in Native American Communities. Current Environmental Health Reports, 4(2), 130–141. 10.1007/s40572-017-0140-5 [PubMed: 28447316]

Li W, Zhang M, Wang M, Han Z, Liu J, Chen Z, … Liu Z (2018). Screening of groundwater remedial alternatives for brownfield sites: a comprehensive method integrated MCDA with numerical simulation. Environmental Science and Pollution Research, 25(16), 15844–15861. 10.1007/s11356-018-1721-z [PubMed: 29582330]

Lindsey CG, Chen J, Dye TS, Richards LW, & Blumenthal DL (1999). Meteorological Processes Affecting the Transport of Emissions from the Navajo Generating Station to Grand Canyon National Park. Journal of Applied Meteorology, 38(8), 1031–1048. 10.1175/1520-0450(1999)038<1031:MPATTO>2.0.CO;2

Lowe AA, Bender B, Liu AH, Solomon T, Kobernick A, Morgan W, & Gerald LB (2018). Environmental Concerns for Children with Asthma on the Navajo Nation. Annals of the American Thoracic Society, 15(6), 745–753. 10.1513/AnnalsATS.201708-674PS [PubMed: 29485894]

Malczewski J (2006a). GIS-based multicriteria decision analysis: A survey of the literature. International Journal of Geographical Information Science, 20(7), 703–726. 10.1080/13658810600661508

Malczewski J (2006b). Ordered weighted averaging with fuzzy quantifiers: GIS-based multicriteria evaluation for land-use suitability analysis. International Journal of Applied Earth Observation and Geoinformation, 8(4), 270–277. 10.1016/j.jag.2006.01.003

McNeley JK (1981). Holy Wind in Navajo Philosophy - James Kale McNeley - Google Books. Retrieved from https://books.google.com/books?id=RwndbkYQUfkC&dq=navajo+nation+wind&lr=&source=gbs_navlinks_s

Paquette J, & Lowry J (2012). Flood hazard modelling and risk assessment in the Nadi River Basin, Fiji, using GIS and MCDA. The South Pacific Journal of Natural and Applied Sciences, 30(1), 33 10.1071/SP12003

Rangel-Buitrago N, & Anfuso G (2015). Review of the Existing Risk Assessment Methods. In Rangel-Buitrago N & Anfuso G (Eds.), Risk Assessment of Storms in Coastal Zones: Case Studies from Cartagena (Colombia) and Cadiz (Spain) (pp. 7–13). 10.1007/978-3-319-15844-0_2

Rock T (2017). Developing Policy around Uranium Contamination on the Navajo Nation Using Traditional Ecological Knowledge (Doctoral Dissertation). Northern Arizona University, Flagstaff, AZ.

Ryan PH, LeMasters GK, Levin L, Burkle J, Biswas P, Hu S, … Reponen T (2008). A land-use regression model for estimating microenvironmental diesel exposure given multiple addresses

from birth through childhood. Science of The Total Environment, 404(1), 139–147. 10.1016/j.scitotenv.2008.05.051 [PubMed: 18625514]

Saaty TL (1977). A scaling method for priorities in hierarchical structures. Journal of Mathematical Psychology, 15(3), 234–281. 10.1016/0022-2496(77)90033-5

Sherry JW (2002). Land, Wind, and Hard Words: A Story of Navajo Activism. Retrieved from https://books.google.com/books?id=1B2r7wyQYGUC&dq=navajo+nation+wind&lr=&source=gbs_navlinks_s

U.S. Census Bureau. (n.d.). American FactFinder. Retrieved July 2, 2019, from American FactFinder website: https://factfinder.census.gov/faces/nav/jsf/pages/searchresults.xhtml?refresh=t

U.S. Environmental Protection Agency. (2006). Abandoned Uranium Mines and the Navajo Nation: Navajo Nation AUM Screening Assessment Report and Atlas with Geospatial Data. San Francisco, CA.

U.S. Geological Survey. (1975). National Uranium Resource Evaluation (NURE) Hydrogeochemical and Stream Sediment Reconnaissance data [Dataset]. Denver, CO.

U.S. Geological Survey. (n.d.). EarthExplorer - Home. Retrieved June 20, 2019, from EarthExplorer website: https://earthexplorer.usgs.gov/

Yang J, Teng Y, Song L, & Zuo R (2016). Tracing Sources and Contamination Assessments of Heavy Metals in Road and Foliar Dusts in a Typical Mining City, China. PLOS ONE, 11(12), e0168528 10.1371/journal.pone.0168528 [PubMed: 27992518]

Yen J, & Langari R (1999). Fuzzy logic: Intelligence, control, and information. Upper Saddle River, N.J.: Prentice Hall, c1999. (Centennial Lower Level 2 QA9.64 Y46 1999).

Young J, Rinner C, & Patychuk D (2010). The Effect of Standardization in Multicriteria Decision Analysis on Health Policy Outcomes In Phillips-Wren G, Jain LC, Nakamatsu K, & Howlett RJ (Eds.), Advances in Intelligent Decision Technologies (pp. 299–307). Springer Berlin Heidelberg.

Yudego EA, Candás JL, Álvarez EÁ, López MJ, García L, & Fernández-Pacheco VM (2018). Computational Tools for Analysing Air Pollutants Dispersion: A Comparative Review. In Multidisciplinary Digital Publishing Institute Proceedings (Vol. 2, No. 23, p. 1408).

Zadeh LA (1965). Fuzzy sets. Information and Control, 8(3), 338–353. 10.1016/S0019-9958(65)90241-X

Zychowski KE, Kodali V, Harmon M, Tyler CR, Sanchez B, Ordonez Suarez Y, … Campen MJ (2018). Respirable Uranyl-Vanadate-Containing Particulate Matter Derived From a Legacy Uranium Mine Site Exhibits Potentiated Cardiopulmonary Toxicity. Toxicological Sciences, 164(1), 101–114. 10.1093/toxsci/kfy064 [PubMed: 29660078]

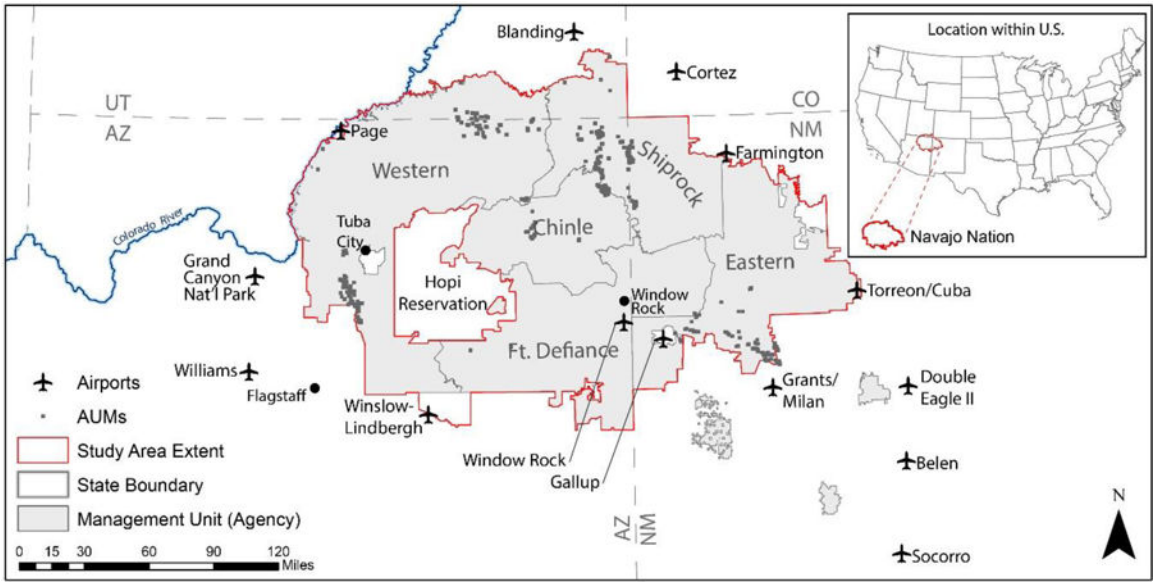

Figure 1.

Study area map showing administrative agencies, AUMs, and airports within the Navajo Nation, located in the southwest United States. Agencies are numbered as 1) Western, 2) Northern, 3) Central, 4) Eastern, and 5) Ft. Defiance

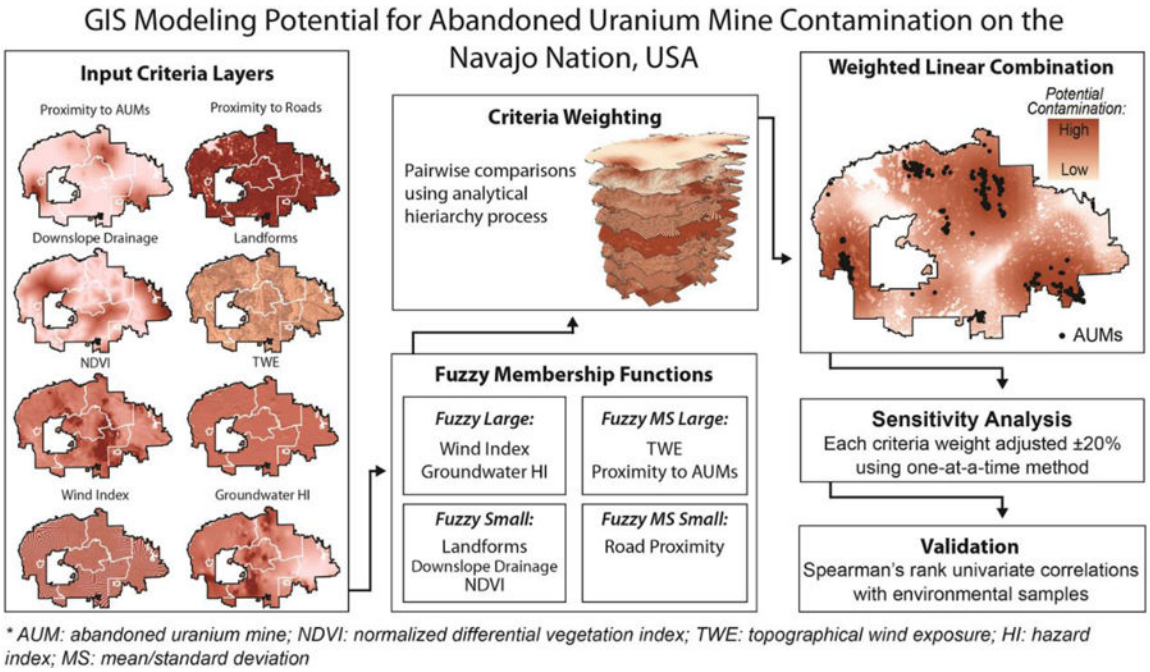

Figure 2.
Methodology framework

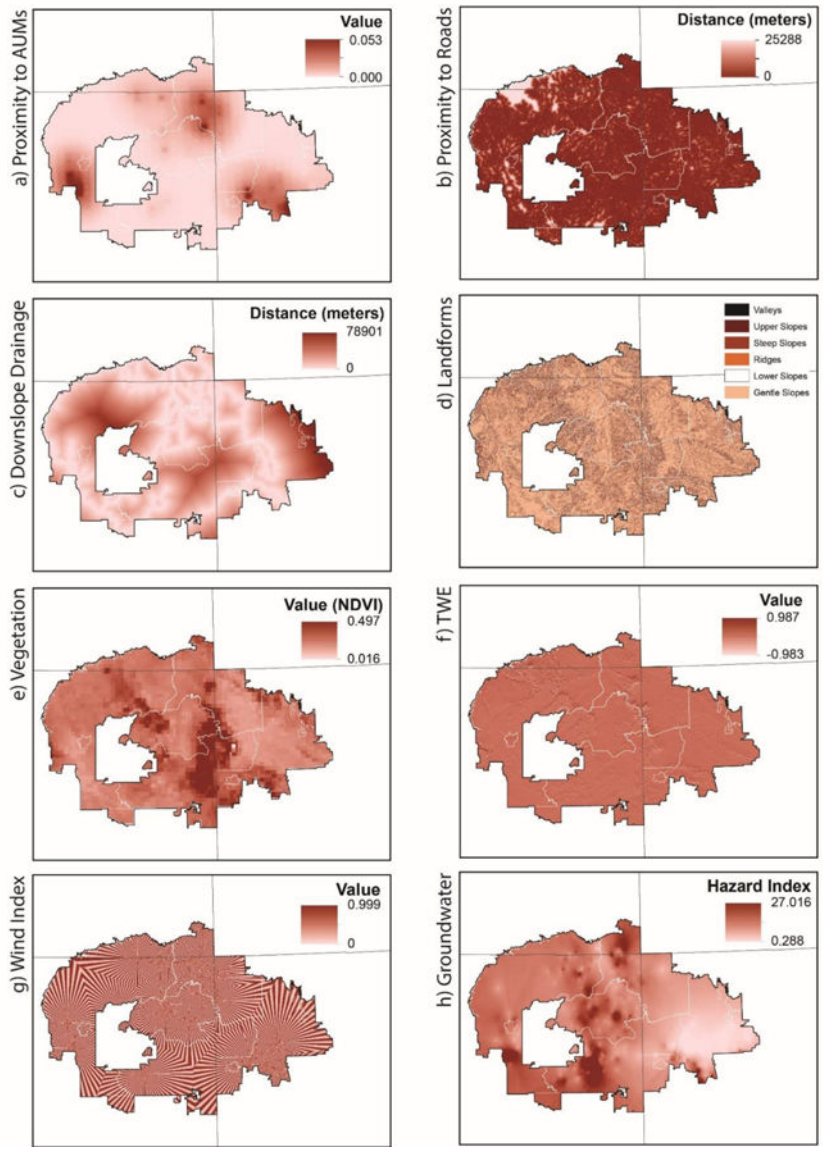

Figure 3.

Criteria maps generated prior to fuzzification: a) proximity to AUMs, b) proximity to roads, c) proximity to downslope drainage, d) landforms, e) vegetation, f) topographic wind exposure (TWE), g) wind index, h) groundwater contamination. Maps of vegetation, TWE, and wind index are generated from data for the month of April.

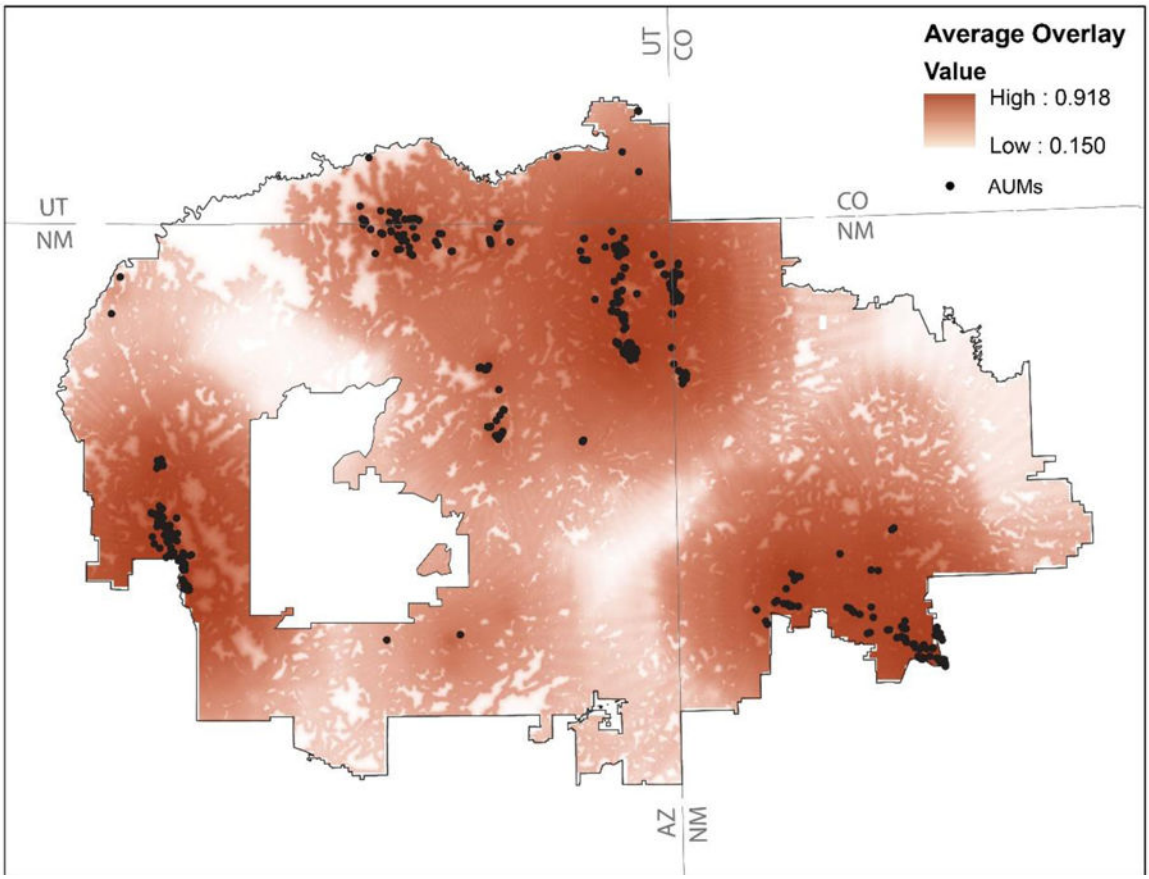

Figure 4.
Composite environmental risk map illustrating potential AUM contamination as the average of all monthly risk surfaces

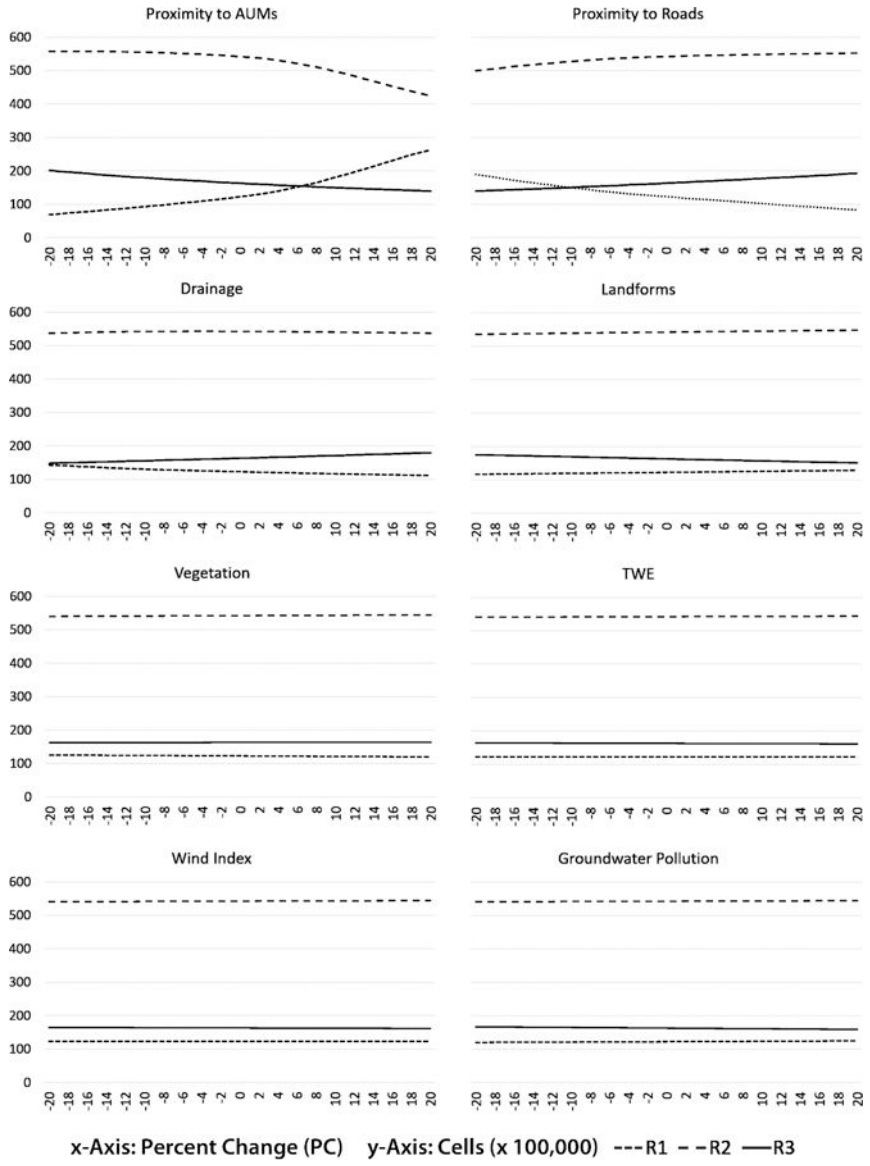

Figure 5.

Summary results from 320 simulation runs (40 per criteria layer) (low risk (R1), medium risk (R2), and high risk (R3))

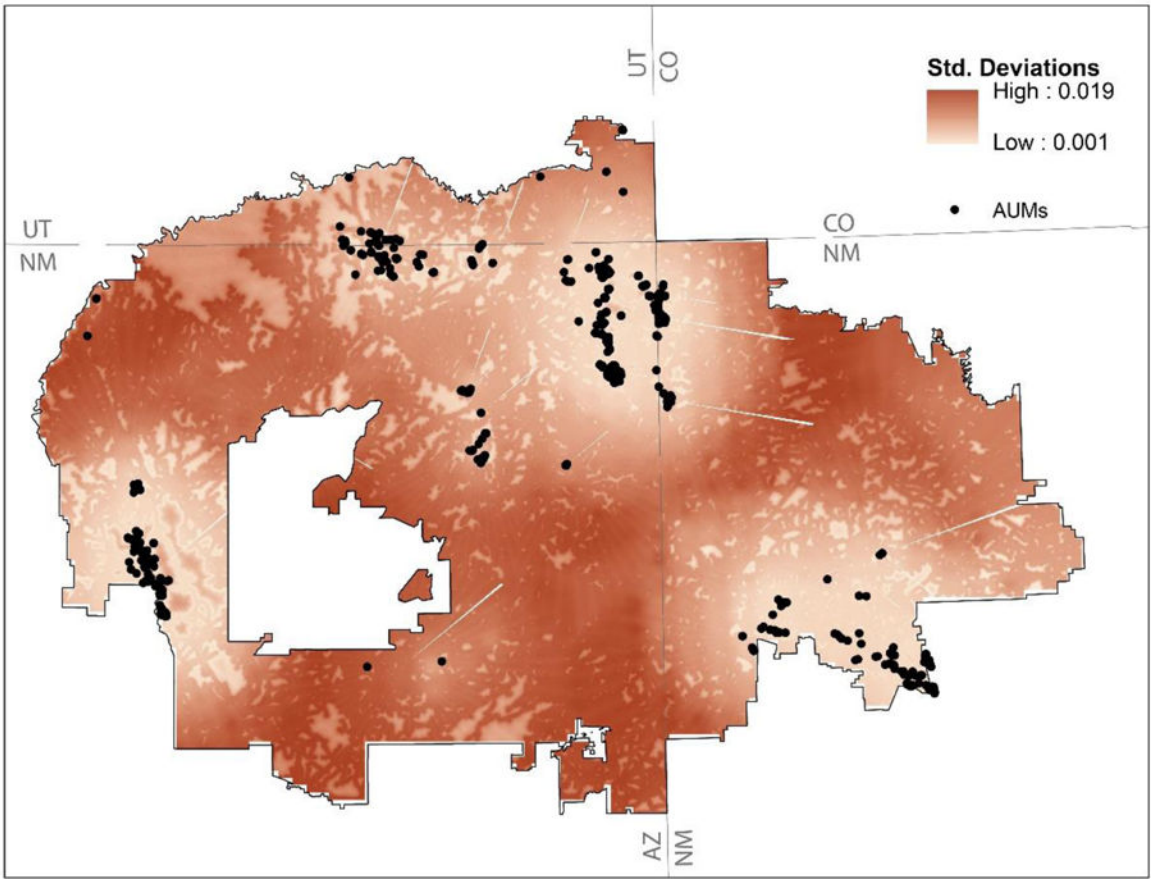

Figure 6.
Standard deviations of risk scores from all 320 simulation runs in April

Table 1

Fuzzy function, midpoint, and spread for each factor layer used to create the environmental risk map

Factor	Fuzzy Function	Midpoint (Spread)*
Proximity to AUMs	MS large	0.269 (1)*
Proximity to roads	MS small	1 (1)*
Downslope drainage	Small	39,530.762 (10)
Landforms	Small	1.5 (3)
Wind Index	Large	0.499 (2)
TWE	MS large	1 (0.025)*
Vegetative robustness	Small	3,231.5 (2)
Groundwater contamination	Large	13.652 (5)

* **Note:** indicates mean (standard deviation)

Table 2

Descriptive statistics of fuzzy membership scores for the criteria layers

	Proximity AUMs	Proximity Roads	Drainage	Landforms	Vegetation*	TWE*	WI*	GW
Min	0.000	0.055	0.001	0.111	0.211	0.000	0.000	0.000
Average	0.292	0.917	0.893	0.135	0.674	0.458	0.439	0.002
Max	0.923	1.000	1.000	1.000	0.996	0.988	0.8	0.968
Std. Dev.	0.243	0.179	0.262	0.068	0.133	0.469	0.31	0.016

*Note. Criterion calculated using April values

AUM: abandoned uranium mines; TWE: topographic wind exposure; WI: wind index; GW: groundwater

Table 3

Pairwise comparison decision matrix for factors from AHP

Categories:	Prox	Roads	Drainage	Landform	Veg	TWE	WI	GW	Weights
Proximity to AUM	1	5	6	7	8	9	9	9	0.441
Roads	1/5	1	4	6	7	7	8	8	0.239
Drainage	0.17	1/4	1	4	5	6	6	6	0.134
Landforms	0.14	0.17	1/4	1	3	4	4	5	0.072
Vegetation	0.12	0.14	1/5	1/3	1	2	3	3	0.041
TWE	0.11	0.14	0.17	1/4	1/2	1	2	2	0.029
Wind index	0.11	0.12	0.17	1/4	1/3	1/2	1	2	0.024
Groundwater pollution	0.11	0.12	0.17	1/5	1/3	1/2	1/2	1	0.020

Table 4

Validation results (R^2) between all monthly surfaces and NURE sediment samples and ASEPCT data

	Jan	Feb	Mar	Apr	May	Jun	Jul	Aug	Sep	Oct	Nov	Dec
ASPECT	0.848	0.846	0.847	0.844	0.845	0.844	0.844	0.845	0.847	0.846	0.846	0.846
NURE	0.955	0.954	0.955	0.955	0.955	0.955	0.954	0.954	0.955	0.954	0.955	0.954